PCCP

RSC Publishing

PAPER

View Article Online
View Journal | View Issue

Highly soluble energy relay dyes for dye-sensitized solar cells†

Cite this: *Phys. Chem. Chem. Phys.*, 2013, **15**, 11306

George Y. Margulis,‡[a] Bogyu Lim,‡[b] Brian E. Hardin,[c] Eva L. Unger,[b] Jun-Ho Yum,[d] Johann M. Feckl,[e] Dina Fattakhova-Rohlfing,[e] Thomas Bein,[e] Michael Grätzel,[d] Alan Sellinger*[f] and Michael D. McGehee*[b]

Received 8th March 2013,
Accepted 24th May 2013

DOI: 10.1039/c3cp51018b

www.rsc.org/pccp

High solubility is a requirement for energy relay dyes (ERDs) to absorb a large portion of incident light and significantly improve the efficiency of dye-sensitized solar cells (DSSCs). Two benzonitrile-soluble ERDs, BL302 and BL315, were synthesized, characterized, and resulted in a 65% increase in the efficiency of TT1-sensitized DSSCs. The high solubility (180 mM) of these ERDs allows for absorption of over 95% of incident light at their peak wavelength. The overall power conversion efficiency of DSSCs with BL302 and BL315 was found to be limited by their energy transfer efficiency of approximately 70%. Losses due to large pore size, dynamic collisional quenching of the ERD, energy transfer to desorbed sensitizing dyes and static quenching by complex formation were investigated and it was found that a majority of the losses are caused by the formation of statically quenched ERDs in solution.

1. Introduction

Dye-sensitized solar cells (DSSCs) are drawing a large amount of attention for their relatively high efficiencies, simple and low-cost processing conditions, and aesthetic appearance.[1–3] Efficiencies have consistently increased, with ruthenium, porphyrin, and organic dyes all achieving greater than 10% efficiency under the simulated AM1.5G solar spectrum, and record efficiencies surpassing 12%.[4–6] An ideal sensitizer would have a broad, strong absorption across the visible and near infrared wavelengths, but typically dyes are unable to effectively cover the entire desired spectrum.[7,8] In addition to functioning as the primary absorber in the DSSC, the sensitizing dye has a myriad of other responsibilities, including rapid electron injection,[9,10] efficient hole regeneration,[11,12] and acting as an effective barrier to recombination.[13–15] A variety of multiple dye solutions has been utilized to achieve strong and broad absorption, including cosensitization,[16,17] cosensitized energy transfer,[18–20] dyadic sensitizers,[21,22] and energy relay dyes (ERDs).[23–27] These approaches have been extremely successful, with the aforementioned record efficiency being achieved in a dual dye cosensitized system.[4]

Energy relay dyes are dissolved dyes within the electrolyte that, upon excitation, undergo Förster resonance energy transfer (FRET) to the sensitizing dye.[23,28] ERDs have the advantage of separating the responsibilities of recombination blocking and charge injection from the function of light absorption. Hence, using multiple ERDs to cover the solar spectrum in conjunction with an efficient, highly performing sensitizing dye can be a strategy toward highly efficient DSSCs.[29] Additionally, there is little effort required to optimize a DSSC utilizing an ERD, as the ERD is simply added to the electrolyte with no other changes in the device fabrication. Previous work has shown that ERDs can transfer energy to the sensitizing dye with near 100% efficiency.[30] Until now, the poor solubility of ERDs has limited performance due to the inability of the ERD to absorb most of the incident photons. As the thickness and porosity of typical nanoporous electrodes used in DSSCs is approximately 6 μm and 0.5, respectively, ERDs must be able to achieve an optical density of at least 1 in an effective thickness of only 3 μm.

[a] *Department of Applied Physics, Stanford University, McCullough Building, 476 Lomita Mall, Stanford, CA, 94305, USA*
[b] *Department of Materials Science and Engineering, Stanford University, McCullough Building, 476 Lomita Mall, Stanford, CA, 94305, USA. E-mail: mmcgehee@stanford.edu*
[c] *The Molecular Foundry, Lawrence Berkeley National Laboratory, 67 Cyclotron Road, Berkeley, CA, 94720, USA*
[d] *Laboratory of Photonics and Interfaces, École Polytechnique Fédérale de Lausanne, 1015 Lausanne, Switzerland. E-mail: michael.graetzel@epfl.ch*
[e] *Department of Chemistry and Center for NanoScience (CeNS), Ludwig-Maximilians-Universität München, Butenandtstr. 5–13 (E), Gerhard-Ertl-Building, München, 81377, Germany. E-mail: bein@lmu.de*
[f] *Department of Chemistry and Geochemistry, Colorado School of Mines, Coolbaugh Hall, 1012 14th Street, Golden, CO 80401, USA. E-mail: aselli@mines.edu*

† Electronic supplementary information (ESI) available. See DOI: 10.1039/c3cp51018b

‡ These authors contributed equally to this work.

While ERDs no longer perform the functions of efficiently injecting charge and blocking recombination, they carry with them another set of design rules. Effective long range FRET from ERD to sensitizing dye requires a large Förster radius and excellent photoluminescence efficiency.[31] In addition, the various ions in the redox electrolyte can cause photoluminescence quenching of the excited ERD leading to lost energy. Finally, the ERD must be extremely soluble in one of the various solvents used in the electrolyte of DSSCs.

2. Dye structure and device results

Two dyes were designed for use as ERDs in DSSCs, coded BL302 and BL315, with chemical structures depicted in Fig. 1. Both BL302 and BL305 are similar in structure to the common laser dye DCM (4-(dicyanomethylene)-2-methyl-6-(*p*-dimethylaminostyryl)-4*H*-pyran, also depicted in Fig. 1 for comparison), which has shown efficient energy transfer in DSSCs.[30] Through the use of additional alkyl and alkoxy groups, both dyes display excellent solubilities of approximately 180 mM in benzonitrile. BL302 has an absorption and photoluminescence spectrum nearly identical to that of DCM, while BL315 shows a slightly redshifted absorption and emission spectrum due to the insertion of a thiophene moiety into the dye (Fig. S3 in the ESI†). Both dyes show good complementary absorption with TT1, a strongly absorbing, zinc-pthalocyanine-based sensitizer.[32,33] Additionally, the emission spectra of BL302 and BL315 show sufficient spectral overlap with the absorption spectrum of TT1 (see Fig. S6 in the ESI†), resulting in large FRET radii of approximately 6 nm and 5 nm, respectively. Previously performed calculations show that these FRET radii for BL302 and BL315 should allow for high (greater than 95%) energy transfer in the 17–20 nm pores typically used in DSSCs.[31]

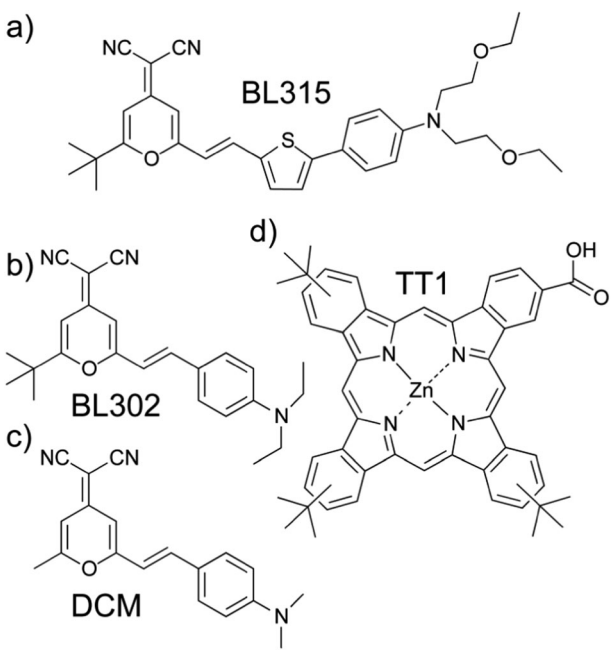

Fig. 1 Chemical structure of dyes. Energy relay dyes: (a) BL315, (b) BL302, (c) DCM. Sensitizing dye: (d) TT1.

Table 1 *J–V* characteristics for TT1 devices incorporating BL302 and BL315 as an ERD. *J–V* curves are shown in the ESI (Fig. S16)

Device	J_{SC} (mA cm^{-2})	V_{OC} (V)	FF	Efficiency (%)
Reference	6.0	623	0.67	2.51
20 mM BL302	7.1	618	0.68	2.99
60 mM BL302	8.7	619	0.64	3.47
180 mM BL302	9.7	640	0.62	3.80
20 mM BL315	7.3	633	0.67	3.05
60 mM BL315	9.4	633	0.62	3.69
180 mM BL315	10.8	640	0.60	4.14

TT1-sensitized DSSCs were fabricated as previously reported, using varying concentrations of BL302 or BL315 dissolved in a benzonitrile-based electrolyte. The full device fabrication procedure is contained in the ESI.†

As shown in Table 1, BL302 and BL315 both significantly improve the efficiency of the reference device, particularly due to a strong increase in the short-circuit photocurrent density (J_{SC}). While the fill factor (FF) does decrease slightly, this is not necessarily caused by the ERD, as increasing the photocurrent of a solar cell typically lowers the fill factor. Impedance spectroscopy has been used to investigate the various charge transport processes occurring within a DSSC, including mass transport of the electrolyte.[34] To see if high concentrations of ERD affected the diffusion of the redox species within the DSSC, impedance measurements were performed at a forward bias of 0.8 V, (Fig. S14 in the ESI†). It was observed that there is little change in the diffusion of the I^-/I_3^- redox shuttle with or without 180 mM of the BL302 ERD, confirming that mass transport of the redox shuttle is relatively unaffected by high concentrations of ERD. Overall, BL315 results in a 65% increase in efficiency of the TT1 DSSC, while BL302 increases device performance by 51%.

The external quantum efficiency (EQE) of the DSSCs is shown in Fig. 2. The superior photovoltaic performance of BL315 as compared to BL302 can be attributed to its broader, more red-shifted absorption. However, despite the high dye loading, the EQE in the ERD portion of the spectrum (450–550 nm) is still significantly lower than the peak EQE of the TT1 sensitizing dye. Conversion of incident photons into collected charges by an ERD is a three-step process, and the EQE of the ERD (EQE_{ERD}) can be written as

$$EQE_{ERD} = ABS_{ERD} \times ETE \times IQE_{SD}, \quad (1)$$

where ABS_{ERD} is the absorptance of the ERD within the mesoporous TiO_2 layer (fraction of photons absorbed by the ERD), ETE is the energy transfer efficiency of the ERD to the sensitizing dye, and IQE_{SD} is the internal quantum efficiency (IQE) of the sensitizer. The absorptance of the ERD can be estimated from Beer's law:

$$ABS_{ERD} = T_{FTO}[1 - \exp(-\rho c \alpha x)], \quad (2)$$

where T_{FTO} is the transmission through the FTO electrode (measured to be 0.91 at 520 nm, see Fig. S7 in the ESI†), ρ and x are the porosity and thickness of the TiO_2 mesoporous layer (approximately 0.5 and 6 μm, respectively), c is the concentration

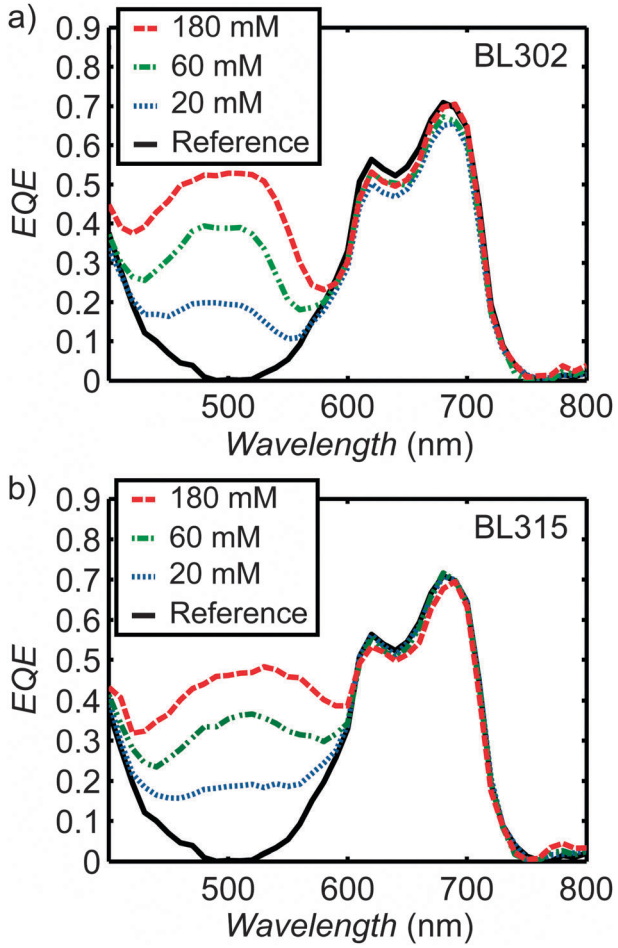

Fig. 2 EQE of 6 μm-thick TT1-sensitized DSSCs containing various amounts of BL302 (a) and BL315 (b) in the electrolyte.

of the ERD, and α is the molar extinction coefficient of the ERD (30 000 M^{-1} cm^{-1} at 520 nm for BL302). For 180 mM BL302, this absorptance comes out to 0.89 at 520 nm, meaning nearly all available light transmitted through the FTO is absorbed by the ERD. While it is possible that the concentration of the ERD within the TiO_2 pores is less than the average concentration within the electrolyte, the high absorptance of the ERD means that even for a significant change in the ERD concentration, ABS_{ERD} remain near 0.91. The flattening of the EQE in the ERD portion of the spectrum in Fig. 2 with increasing dye concentration suggests that indeed the absorption is saturating.

The IQE of the sensitizer can be computed by dividing the EQE of the sensitizer (EQE_{SD}) by the percentage of photons absorbed by the sensitizer (ABS_{SD}):

$$IQE_{SD} = \frac{EQE_{SD}}{ABS_{SD}}. \quad (3)$$

While technically EQE_{SD} and ABS_{SD} vary as a function of wavelength, IQE_{SD} is relatively independent of wavelength for the TT1 DSSCs, and using the peak absorptance and EQE of TT1 allows for an accurate measurement of the IQE (see Fig. S8 in the ESI†). After calculating IQE_{SD} and ABS_{ERD}, the ETE can be calculated from the measured energy relay dye EQE and eqn (1). While previously ETE's for DCM to TT1 have been shown to be in excess of 90%,[30] the average ETE for BL302 to TT1 is only approximately 70%, and the corresponding ETE for BL315 is approximately 67%. ETE calculations were performed at 520 nm rather than the dye absorption peak wavelength to ensure the absorption of the sensitizer and electrolyte were small.

3. Analysis of ETE losses

3.1. Introduction to loss mechanisms

ETE losses can be caused by a variety of physical processes in the DSSC, and before analyzing which process contributes the most to the 30% losses seen with BL302, it is instructive to give a brief overview of the ways ERD excitations can be lost. FRET between two chromophores is a short scale interaction that can only occur efficiently over distances of 1–10 nm. If the pore size is too large, then the ERD cannot efficiently transfer energy to the sensitizing dye and the excitation is lost. The theoretical energy transfer efficiency of ERDs in pores has been previously simulated.[31] Dynamic (collisional) quenching of the chromophore in solution is a competing process with FRET, and the effects of dynamic quenching are included in the calculations of ERD ETE as a function of pore size. On the other hand, static quenching, such as quenching from forming a non-emissive complex in solution, results in 'dead dyes' that cannot energy transfer to sensitizers. Thus, static quenching results in a complete loss of excitation, rather than a competing rate process. Finally, the ERD can energy transfer to a dye that is no longer attached to the TiO_2 surface. Such a desorbed dye will be unable to inject charge, and the excitation of the ERD will be lost. Considering these three possibilities allows for an understanding of the dominant loss mechanism of BL302 excitation in DSSCs.

3.2. Pore size dependence

As mentioned previously, energy transfer can be highly dependent on the TiO_2 pore size. Devices were fabricated using substrates with 3 average pore sizes: 12 nm, 17 nm and 32 nm.[4,35,36] Average ETE values for these devices are displayed in Fig. 3 along with theoretical ETE values. The energy transfer efficiency for an ERD can be calculated based on the dynamic quenching rate, FRET radius, and the sensitizing dye surface coverage for various pore geometries.[31] Based on the dynamic quenching rate of BL302 in the electrolyte, (Fig. S9 in the ESI†) the calculated FRET radius of 6 nm, and estimated dye coverage of 1 nm^{-2}, the simulated ETE can be calculated as shown in Fig. 3. Even at a pore radius of 32 nm, the expected ETE inside a spherical pore is 94%; however, the experimentally seen ETE remains significantly lower – relatively constant near approximately 70%. This suggests that the pore size is not a significant factor in the incomplete energy transfer efficiency and that ERDs are compatible with a variety of pore sizes, including the larger nanopores implemented in current record devices.[4]

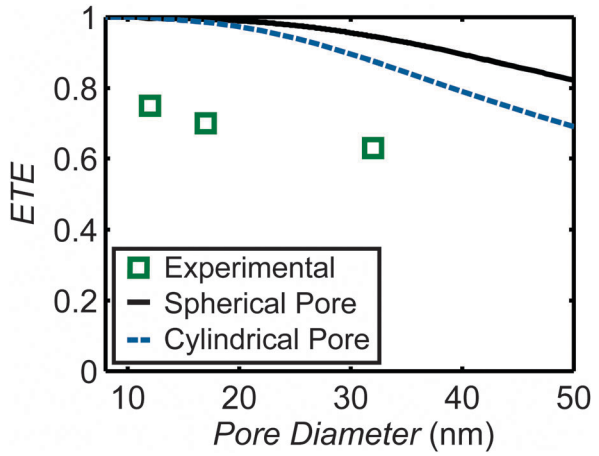

Fig. 3 Experimental ETE compared to expected theoretical ETE for spherical and cylindrical pore geometries.

3.3. Dye desorption losses

Benzonitrile was used as an electrolyte solvent due to its relative stability, lower vapor pressure and enhanced solubility of alkyl-substituted ERDs versus the commonly used acetonitrile. Benzonitrile also enhances the solubility of the sensitizing dye, since sensitizing dyes often use alkyl groups to help prevent recombination at the titania interface.[13–15] To quantify the amount of TT1 desorption, a sandwich device was fabricated exactly like a DSSC except substituting a plain glass electrode for the Pt-counter-electrode (inset of Fig. 4). The sandwich device was then filled with benzonitrile or acetonitrile electrolyte and left for a week for the dye desorption–adsorption processes to equilibrate. Over the course of a week, the electrolyte turned a slightly blue color due to desorbed dyes from the TiO_2 surface. The absorption was measured through a region of the sandwich device that contained no TiO_2, but had electrolyte with desorbed dye electrode (inset of Fig. 4). Using the known width of the surlyn spacer, this gives an estimate of the desorbed dye concentration within the electrolyte and hence the desorbed dye concentration within the TiO_2 pores.

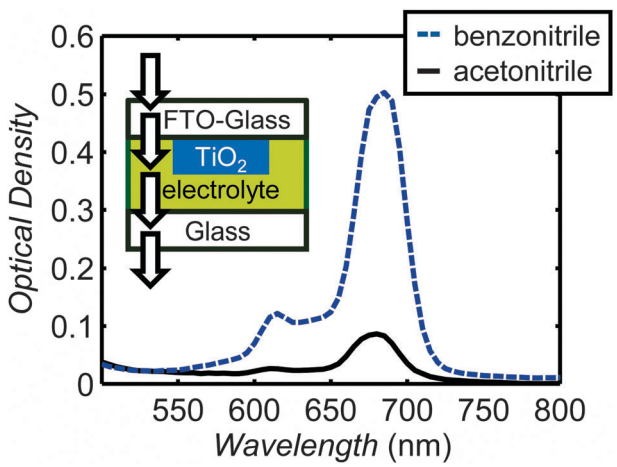

Fig. 4 Absorption of electrolyte after equilibration of dye desorption for benzonitrile and acetonitrile based electrolytes. Inset: experimental schematic of measuring light absorption through the electrolyte. After allowing dye desorption to equilibrate, the absorption of the dye in the electrolyte is measured using a beam path shown by the arrows in the inset.

As shown in Fig. 4, only a small amount of sensitizing dye desorbs into the acetonitrile electrolyte, while benzonitrile causes an approximately 6× increase in concentration of TT1 within the electrolyte. At equilibrium the measured concentration in the acetonitrile and benzonitrile electrolytes is 0.23 mM and 1.31 mM, respectively. It should be noted that these concentrations correspond to a small fraction of the TiO_2 adsorbed dyes and hence doesn't greatly affect the density of dyes on the surface. Assuming that this dye concentration is present within the pores, this corresponds to approximately 2.0 dye molecules contained in a 17 nm spherical pore for a DSSC using benzonitrile electrolyte. Because of the r^{-6} dependence of the FRET rate on the chromophore separation distance (r), ERDs within the neighborhood of the desorbed dye can preferentially energy transfer to the desorbed dye. This can be simulated by placing a desorbed dye at a given distance from the center of the pore and calculating the relative FRET rates to the desorbed dye and to the attached sensitizing dyes on the TiO_2 surface. From these rates and the assumption of homogeneous ERD distribution within the pores, the ETE loss as a function of desorbed ERD distance from the center of the pore can be calculated, and is shown in Fig. S11 in the ESI.† The ETE loss for 1 desorbed dye in the center of the pore is approximately 3.5%, but becomes less if the desorbed dye is at a position away from the pore center. Assuming the desorbed dye is not within 2 nm of the pore surface (to account for the physical space of the sensitizing dyes on the surface), the average ETE loss per desorbed dye can be calculated to be 1.8%. Thus, the loss due to dye desorption in a 17 nm pore is approximately 3.6%. While this loss is an important consideration, it does not explain the entire 30% ETE loss seen in the BL302 devices.

3.4. Static dye quenching

FRET to an ERD occurs at a certain rate based on the distance between chromophores and their FRET radius. In a DSSC, there are competing rate processes, such as dynamic (collisional) quenching of the excitation by the various ions in the electrolyte. If the FRET rate is significantly faster than this dynamic quenching rate, then the ETE can still approach unity. On the other hand, if the dye is statically quenched, through a process such as forming a nonemissive complex in solution, the complex no longer has an opportunity to FRET to a sensitizing dye on the TiO_2 surface, and the excitation is lost.[37] In order to investigate the losses due to of static quenching of the ERD, steady-state and time-resolved photoluminescence (PL) quenching experiments were performed. During a steady-state PL measurement, both dynamic quenching and static quenching cause a decrease in the PL signal. However, during time-resolved PL quenching measurements, a decrease in the PL lifetime can only be caused by a change in the dynamic quenching rate – non-emissive statically-quenched complexes simply do not photoluminesce. Thus by comparing the steady-state PL quenching and decrease in PL lifetime, the amount of static

and dynamic PL quenching can be calculated.[37] The steady state PL quenching should be given by

$$\mathrm{PL} = \frac{(1-r)\mathrm{PL}_0}{\tau_0/\tau}, \quad (4)$$

where r is the fraction of dyes that are statically quenched, PL and PL_0 are the magnitudes of the steady state photoluminescence with and without addition of the quenchers, respectively, and τ and τ_0 are the PL lifetimes with and without quenchers, respectively. A comparison of the time-resolved and steady-state PL measurements of BL302 as a function of electrolyte concentration is shown in Fig. 5a.

As can be seen in Fig. 5a, there is significantly more steady-state PL quenching than can be explained by the decrease in PL lifetime. While both $\mathrm{PL}_0/\mathrm{PL}$ and τ_0/τ display linear trends, the decrease in the steady-state photoluminescence is larger than the decrease in photoluminescence lifetimes, even at low electrolyte concentrations. This data suggests that BL302 is being statically quenched, possibly by forming complexes with components of the electrolyte. By measuring the quenching at 100% electrolyte concentration for 10 mM BL302, $\mathrm{PL}_0/\mathrm{PL}$ and τ_0/τ were found to be 3.0 and 2.0, respectively. Applying eqn (4), it is found that r, the fraction of statically quenched dyes, is approximately 0.33 in the conditions present in the DSSC. While this number is larger than the 25–30% losses that are seen for the BL302 devices, it is important to note that statically quenched dyes can still contribute to photocurrent by direct injection. As has been previously seen,[30] ERDs are able to inject and generate photocurrent even in the absence of sensitizing dyes, albeit at a much lower efficiency than by FRET. Thus, while a small portion of the statically quenched dyes may directly inject and their excitations are not lost, static quenching can explain the 26% of the ETE loss that is unaccounted for by energy transfer to desorbed dyes.

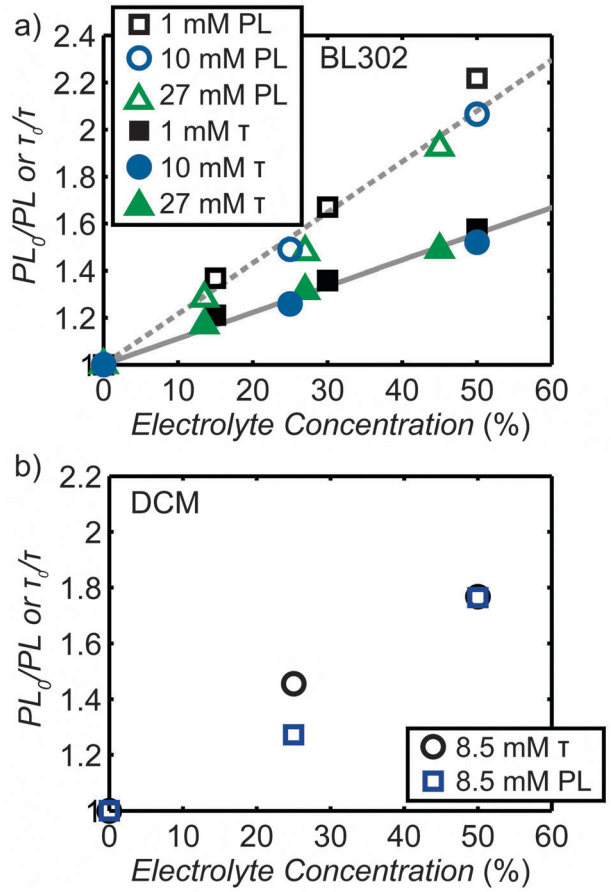

Fig. 5 (a) Comparison of steady-state photoluminescence quenching with decrease in photoluminescence lifetime for 1 mM, 10 mM, and 27 mM BL302 with varying concentrations of electrolyte. Solid and dashed grey lines are linear fits of PL and τ, respectively. Note: the linear trend continues for both PL and τ to 100% electrolyte concentration. (b) Comparison of steady-state photoluminescence quenching with decrease in photoluminescence lifetime for DCM dye in electrolyte. Note: electrolyte concentration (%) is the percentage of electrolyte components relative to the standard electrolyte used in DSSC devices.

As shown in Fig. 5b, static quenching by the electrolyte does not occur for DCM in either benzonitrile-based or acetonitrile-based (Fig. S12 in the ESI†) electrolytes. The difference in quenching between BL302 and DCM could originate from the difference in their structure. Compared to DCM, BL302 has different length alkyl chains on the amine group and a change from a methyl to a bulkier *tert*-butyl substituent group on the pyran ring. This could lead to a different coordination with the electrolyte components,[38] possibly with formation of a non-emissive complex within the pores. Another explanation could be that the increasing amount of ions with electrolyte concentration causes the alkyl-substituted dye molecules to form complexes in solution.

It should be noted that very high concentrations of ERD can also lead to static quenching as the dye is no longer soluble and forms aggregates in solution. Concentration quenching data is shown in Fig. S13 in the ESI.† At high concentrations (180 mM), it can be seen that ERDs are statically quenched by each other, leading to excitation loss. This static concentration quenching may also be a cause of the ETE losses seen with BL302 and BL315 in TT1 DSSCs. However, due to the small size of the pores, larger aggregates caused by lack of solubility may not be able to be formed inside the pores, and it is also possible that any static concentration quenching does not affect DSSC performance.

3.5. ETE losses summary

It has been observed that static quenching (such as by complex formation) is responsible for the majority of BL302 excitation losses. Losses due to desorbed dyes and the large size of TiO_2 nanopores should cause losses of less than 5% in these highly soluble ERD systems, and if dyes can be designed that avoid static quenching, ERDs will be able to achieve the dual goals of both greater than 95% light absorption and 95% energy transfer efficiency.

4. Conclusions

Two highly benzonitrile-soluble ERDs, BL302 and BL315 have been synthesized. While previously ERDs have been unable to achieve near 100% light absorption within the pores of a DSSC,

BL302 and BL315 are able to absorb 97% of the incident light. This results in a 65% increase in the efficiency of a TT1-based DSSC, the highest increase due to an ERD thus far reported. However, BL302 and BL315 only achieve an energy transfer efficiency of approximately 70%, despite the theoretical ETE being very close to 100%. Of this 30% loss, approximately 3.6% can be explained by energy transfer to desorbed sensitizing dyes, while the rest can be explained by static quenching of the ERD. It is hypothesized that quenchers in the electrolyte coordinate to alkyl groups on the soluble ERD, or the introduction of ions causes these ERDs to aggregate. ERDs have drawn interest due to their ease of addition to a DSSC, with significant potential for improving the spectral response of the device. Continuing to gain a better understanding of ERD design rules is necessary for use of ERDs for complementary light harvesting in record devices.

Acknowledgements

This work was supported by the Office of Naval Research (ONR) under grant N000141110244. G.Y.M. would like to acknowledge the support of the ABB Stanford Graduate Fellowship in Science and Engineering. We would like to thank Professor Tomas Torres (Universidad Autónoma de Madrid) for providing TT1 dye.

Notes and references

1 B. O'Regan and M. Grätzel, *Nature*, 1991, **353**, 737–740.
2 A. Hagfeldt, G. Boschloo, L. Sun, L. Kloo and H. Pettersson, *Chem. Rev.*, 2010, **110**, 6595–6663.
3 B. E. Hardin, H. J. Snaith and M. D. McGehee, *Nat. Photonics*, 2012, **6**, 162–169.
4 A. Yella, H.-W. Lee, H. N. Tsao, C. Yi, A. K. Chandiran, M. K. Nazeeruddin, E. W.-G. Diau, C.-Y. Yeh, S. M. Zakeeruddin and M. Grätzel, *Science*, 2011, **334**, 629–634.
5 J.-H. Yum, E. Baranoff, F. Kessler, T. Moehl, S. Ahmad, T. Bessho, A. Marchioro, E. Ghadiri, J.-E. Moser, C. Yi, M. K. Nazeeruddin and M. Grätzel, *Nat. Commun.*, 2012, **3**, 631.
6 M. K. Nazeeruddin, F. De Angelis, S. Fantacci, A. Selloni, G. Viscardi, P. Liska, S. Ito, B. Takeru and M. Grätzel, *J. Am. Chem. Soc.*, 2005, **127**, 16835–16847.
7 S. K. Balasingam, M. Lee, M. G. Kang and Y. Jun, *Chem. Commun.*, 2013, **49**, 1471–1487.
8 H.-P. Wu, Z.-W. Ou, T.-Y. Pan, C.-M. Lan, W.-K. Huang, H.-W. Lee, N. M. Reddy, C.-T. Chen, W.-S. Chao, C.-Y. Yeh and E. W.-G. Diau, *Energy Environ. Sci.*, 2012, **5**, 9843.
9 E. M. Barea, J. Ortiz, F. J. Payá, F. Fernández-Lázaro, F. Fabregat-Santiago, A. Sastre-Santos and J. Bisquert, *Energy Environ. Sci.*, 2010, **3**, 1985.
10 S. E. Koops, B. C. O'Regan, P. R. F. Barnes and J. R. Durrant, *J. Am. Chem. Soc.*, 2009, **131**, 4808–4818.
11 S. Meng and E. Kaxiras, *Nano Lett.*, 2010, **10**, 1238–1247.
12 T. Daeneke, A. J. Mozer, Y. Uemura, S. Makuta, M. Fekete, Y. Tachibana, N. Koumura, U. Bach and L. Spiccia, *J. Am. Chem. Soc.*, 2012, **134**, 16925–16928.
13 J. E. Kroeze, N. Hirata, S. Koops, M. K. Nazeeruddin, L. Schmidt-Mende, M. Grätzel and J. R. Durrant, *J. Am. Chem. Soc.*, 2006, **128**, 16376–16383.
14 L. Schmidt-Mende, J. E. Kroeze, J. R. Durrant, M. K. Nazeeruddin and M. Grätzel, *Nano Lett.*, 2005, **5**, 1315–1320.
15 R. Li, J. Liu, N. Cai, M. Zhang and P. Wang, *J. Phys. Chem. B*, 2010, **114**, 4461–4464.
16 H. Ozawa, R. Shimizu and H. Arakawa, *RSC Adv.*, 2012, **2**, 3198.
17 N. C. Jeong, H.-J. Son, C. Prasittichai, C. Y. Lee, R. A. Jensen, O. K. Farha and J. T. Hupp, *J. Am. Chem. Soc.*, 2012, **134**, 19820–19827.
18 B. E. Hardin, A. Sellinger, T. Moehl, R. Humphry-Baker, J.-E. Moser, P. Wang, S. M. Zakeeruddin, M. Grätzel and M. D. McGehee, *J. Am. Chem. Soc.*, 2011, **133**, 10662–10667.
19 M. Pastore and F. De Angelis, *J. Phys. Chem. Lett.*, 2012, **3**, 2146–2153.
20 M. Shrestha, L. Si, C.-W. Chang, H. He, A. Sykes, C.-Y. Lin and E. W.-G. Diau, *J. Phys. Chem. C*, 2012, **116**, 10451–10460.
21 C. Siegers, J. Hohl-Ebinger, B. Zimmermann, U. Würfel, R. Mülhaupt, A. Hinsch and R. Haag, *ChemPhysChem*, 2007, **8**, 1548–1556.
22 R. Eichberger, C. Strothkämper, I. Thomas, T. Hannappel, K. Schwarzburg, C. Fasting, A. Bartelt and R. Schütz, *J. Photonics Energy*, 2012, **2**, 021003.
23 B. E. Hardin, E. T. Hoke, P. B. Armstrong, J. Yum, P. Comte, T. Torres, J. M. J. Fréchet, M. K. Nazeeruddin, M. Grätzel and M. D. McGehee, *Nat. Photonics*, 2009, **3**, 406–411.
24 G. K. Mor, J. Basham, M. Paulose, S. Kim, O. K. Varghese, A. Vaish, S. Yoriya and C. A. Grimes, *Nano Lett.*, 2010, **10**, 2387–2394.
25 S. Itzhakov, S. Buhbut, E. Tauber, T. Geiger, A. Zaban and D. Oron, *Adv. Energy Mater.*, 2011, **1**, 626–633.
26 E. L. Unger, A. Morandeira, M. Persson, B. Zietz, E. Ripaud, P. Leriche, J. Roncali, A. Hagfeldt and G. Boschloo, *Phys. Chem. Chem. Phys.*, 2011, **13**, 20172–20177.
27 N. Humphry-Baker, K. Driscoll, A. Rao, T. Torres, H. J. Snaith and R. H. Friend, *Nano Lett.*, 2012, **12**, 634–639.
28 J.-H. Yum, B. E. Hardin, S.-J. Moon, E. Baranoff, F. Nüesch, M. D. McGehee, M. Grätzel and M. K. Nazeeruddin, *Angew. Chem., Int. Ed.*, 2009, **48**, 9277–9280.
29 J.-H. Yum, B. E. Hardin, E. T. Hoke, E. Baranoff, S. M. Zakeeruddin, M. K. Nazeeruddin, T. Torres, M. D. McGehee and M. Grätzel, *ChemPhysChem*, 2011, **12**, 657–661.
30 B. E. Hardin, J.-H. Yum, E. T. Hoke, Y. C. Jun, P. Péchy, T. Torres, M. L. Brongersma, K. Nazeeruddin, M. Grätzel, M. D. McGehee and M. K. Nazeeruddin, *Nano Lett.*, 2010, **10**, 3077–3083.
31 E. T. Hoke, B. E. Hardin and M. D. McGehee, *Opt. Express*, 2010, **18**, 3893–3904.

32 J.-J. Cid, J.-H. Yum, S.-R. Jang, M. K. Nazeeruddin, E. Martínez-Ferrero, E. Palomares, J. Ko, M. Grätzel and T. Torres, *Angew. Chem., Int. Ed.*, 2007, **46**, 8358–8362.
33 J.-H. Yum, S.-R. Jang, R. Humphry-Baker, M. Grätzel, J.-J. Cid, T. Torres and M. K. Nazeeruddin, *Langmuir*, 2008, **24**, 5636–5640.
34 F. Fabregat-Santiago, G. Garcia-Belmonte, I. Mora-Seró and J. Bisquert, *Phys. Chem. Chem. Phys.*, 2011, **13**, 9083–9118.
35 J. M. Szeifert, D. Fattakhova-Rohlfing, D. Georgiadou, V. Kalousek, J. Rathouský, D. Kuang, S. Wenger, S. M. Zakeeruddin, M. Grätzel and T. Bein, *Chem. Mater.*, 2009, **21**, 1260–1265.
36 J. M. Szeifert, D. Fattakhova-Rohlfing, J. Rathouský and T. Bein, *Chem. Mater.*, 2012, **24**, 659–663.
37 J. R. Lakowicz, *Principles of Fluorescence Spectroscopy*, Springer, New York, 3rd edn, 2006.
38 X. Li, A. Reynal, P. Barnes, R. Humphry-Baker, S. M. Zakeeruddin, F. De Angelis and B. C. O'Regan, *Phys. Chem. Chem. Phys.*, 2012, **14**, 15421–15428.

